1998

# Applications of the Kubelka-Munk color model to xerographic images

Kristen Hoffman

SIMG-503

Senior Research

# Applications of the Kubelka-Munk Color Model to Xerographic Images

Final Report

Kristen Hoffman

Center for Imaging Science

Rochester Institute of Technology

May 1998

Table of Contents

# Applications of the Kubelka-Munk Color Model to Xerographic Images

Kristen Hoffman

## Table of Contents

## Applications of the Kubelka-Munk Color Model to Xerographic Images

Kristen Hoffman

Advisor: Dr. Edul N. Dalal, Wilson Center for Research and Technology, Xerox Corporation, Webster, N. Y.

# Abstract

The Kubelka-Munk color model describes the reflectance of a color sample as a function of: an absorption spectrum, K (λ ), a scattering spectrum, S(λ
), the sample thickness, X, and the reflectance spectrum of the substrate or backing, $R_p$. For xerographic applications, the existing model has been modified to account for 1) the need to model the reflectance of multi-layer color images, as is the case with many xerographic print samples, 2) the need to apply the color model with correction parameters to images measured using bi-directional measurement geometry, and 3) the variation in toner layer thickness that can occur within a color sample with process xerography. The methods derived to deal with these cases will be outlined as well as results from application of the model to an experimental image set. Color difference (dE*) values between results predicted with the model and measurements made on equivalent samples were used to characterize the accuracy of the model. The average dE* between the color model predictions for single and bi-layer test samples measured with 45/0 bidirectional measurement geometry and actual color measurements on equivalent samples was found to be 1.8 CIELAB units with a corresponding RMS error of 2.1. For single and bi-layer xerographic print samples measured with 45/0 bi-directional measurement geometry, the color difference between color predictions with the model and color measurements of the print samples was found to be 5.1 CIELAB units with a corresponding RMS error of 5.5.

Table of Contents

This report is accepted in partial fulfillment of the requirements of the course SIMG-503 Senior Research.

Title: Applications of the Kubelka-Munk Color Model to Xerographic Images

Author: Kristen Hoffman

Project Advisor: Dr. E. Dalal, Dr. J. Arney

SIMG 503 Instructor: Joseph P. Hornak

Table of Contents

# Introduction

## Kubelka-Munk Color Model

The Kubelka-Munk color model [1, 2, 3]
is a mathematical model used to describe the reflectance of opaque samples. The model considers the absorption and scattering occurring in a colored sample of fixed thickness, and is applied on a wavelength by wavelength basis throughout the visible region of the electromagnetic spectrum. The reflectance of the sample at each wavelength depends on four factors: an absorption spectrum, $K(\lambda)$, a scattering spectrum, $S(\lambda)$, the sample thickness, X, and the reflectance spectrum of the substrate or backing, $R_p(\lambda)$. The model considers the illuminating light to be collimated, and the light penetrating the sample is considered to be scattered. While the light can be scattered in any direction, the model considers two net fluxes: straight up and straight down.

The original Kubelka-Munk color model deals with just one constant colorant layer imaged on top of a backing or substrate. For the purpose of current applications at Xerox, this paper deals with a modification of the model for application to multilayer images, as is the case for many xerographic color print samples. In this paper, the method derived to deal with images with more than one toner layer will be described.

## Saunderson Correction Parameters

Before the Kubelka-Munk model can be applied, a correction has to be made for reflections at the sample surface. A method for making this correction was proposed by Saunderson [4] in terms of two parameters, $k_1$ and $k_2$. The parameter $k_1$ describes the fractional reflectance when light entering the sample is partially reflected at the air-sample interface. Similarly, the parameter $k_2$ describes the fractional reflectance when the light exiting the sample is partially reflected back into the sample at the sample-air interface.

The Saunderson correction was derived for spectrophotometer measurements made with integrating sphere geometry. For the applications of interest in this paper, it was necessary to use a bidirectional (0/45) geometry. It was therefore necessary to derive a modified version of the Saunderson correction incorporating a third parameter, $k_0$, which describes the fraction of light reflected at the air-sample surface which actually reaches the detector. For an integrating sphere geometry with the specular component included, $k_0=k_1$.

## Variations in Toner Layer Thickness

Variations in toner layer thickness across a specific image hinder the accuracy of the Kubelka-Munk color model, which assumes a uniform film thickness throughout a specific sample. Xerographic images can often exhibit toner layers with inconsistent, nonplanar thickness across a particular color patch due to the imaging process. A method has been developed which divides a nonplanar color patch into very small sections so that each section, when viewed individually, appears planar. The Kubelka-Munk color model is then applied to each planar section, and all sections in the entire image are integrated to produce a final reflectance spectrum of the color patch.

# Background and Significance

## 1. Reflection of Color Materials

The color of an object depends on how the object reflects incident light, with respect to wavelength, over the visible region of the electromagnetic light spectrum. The color of a particular object can be predicted if its reflectance with respect to wavelength can be modeled The Kubelka-Munk color model[1, 2, 3] with Saunderson correction parameters[4] models the reflectance of a color sample with respect to wavelength.

## 2. Fresnel Equations

The light reflected by an object consists of two distinct parts: one that is reflected from the object's front surface without ever penetrating into the object, and another that is reflected after having entered the object.

The fraction of the incident light which is reflected from the front surface without ever penetrating into the object is given by Fresnel's law,[3] and is a function of the angle of incidence, $i$, the refractive index of the object, $n_2$, and the refractive index of the surrounding medium, $n_1$. Fresnel's law states that

$$\rho_{\parallel} = \left[\frac{\cos i - \sqrt{(n_2/n_1)^2 - \sin^2 i}}{\cos i + \sqrt{(n_2/n_1)^2 - \sin^2 i}}\right]^2 \quad (1)$$

$$\rho_{\perp} = \left[\frac{(n_2/n_1)^2 \cos i - \sqrt{(n_2/n_1)^2 - \sin^2 i}}{(n_2/n_1)^2 \cos i + \sqrt{(n_2/n_1)^2 - \sin^2 i}}\right]^2 \quad (2)$$

The parallel and perpendicular subscripts refer to the polarization of the incident beam. Equations 1 and 2 can simply be averaged to describe the total reflectance, $\rho_T$, for unpolarized light.

$$\rho_T = \frac{\rho_{\parallel} + \rho_{\perp}}{2} \quad (3)$$

For common dielectric materials having refractive indices of about 1.5 ~ 1.6, approximately 4 to 5% of the incident light is reflected from th front surface. This light maintains the spectral composition of the incident illumination, independent of the color of the object.

## 3. Measurement of Color

A spectrophotometer measures the total reflectance spectrum of an illuminated sample. The CIE tristimulus values of a sample (X, Y, Z) can be calculated[5,6] by multiplying together, wavelength by wavelength, the spectral reflectance of the sample, R(λ ), the relative spectral power distribution of the illuminant, S(λ ), and the tristimulus values of the spectrum colors defining the CIE standard observer. The products are then summed over all the wavelengths in the visible region of the spectrum. Relative power distributions and CIE standard observer functions are predefined. [6] The tristimulus values are defined mathematically as follows:

$$X = 100 \cdot \frac{\sum S(\lambda) \cdot R(\lambda) \cdot \bar{x}(\lambda)}{\sum S(\lambda) \cdot \bar{y}(\lambda)} \quad (4)$$

$$Y = 100 \cdot \frac{\sum S(\lambda) \cdot R(\lambda) \cdot \bar{y}(\lambda)}{\sum S(\lambda) \cdot \bar{y}(\lambda)} \quad (5)$$

$$Z = 100 \cdot \frac{\sum S(\lambda) \cdot R(\lambda) \cdot \bar{z}(\lambda)}{\sum S(\lambda) \cdot \bar{y}(\lambda)} \quad (6)$$

The denominator is a normalizing factor. From the tristimulus values, CIELAB coordinates such as Lightness (L*), Chroma (C*) and Hue Angle (h*) can be calculated to describe the color of a particular sample. Mathematical representations of CIE L*a*b* (CIELAB) color space are as follows:

$$L^* = 116 \cdot \left(\frac{Y}{Y_N}\right)^{\frac{1}{3}} - 16 \quad (7)$$

$$a^* = 500 \cdot \left[\left(\frac{X}{X_N}\right)^{\frac{1}{3}} - \left(\frac{Y}{Y_N}\right)^{\frac{1}{3}}\right] \quad (8)$$

$$b^* = 200 \cdot \left[\left(\frac{Y}{Y_N}\right)^{\frac{1}{3}} - \left(\frac{Z}{Z_N}\right)^{\frac{1}{3}}\right] \quad (9)$$

$$C^* = \sqrt{(a^{*2} + b^{*2})} \quad (10)$$

$$h^* = \arctan\left(\frac{b^*}{a^*}\right) \quad (11)$$

Where $X_N$, $Y_N$, and $Z_N$ are the tristimulus values of a reference neutral white point. Often the reference white point is taken to be a perfectly diffuse reflector, in whi

case $X_N$, $Y_N$, $Z_N$ become merely the tristimulus values of the illuminant. Equations 4, 5 and 6 are valid for values of the ratios $(X/X_N)$, $(Y/Y_N)$, $(Z/Z_N)$ greater than 0.01. If these ratios are less than 0.01, such as for very dark colors, then slightly different equations should be used. [6]

The color difference, Δ E*, between two samples in this color space can be calculated as follows:

$$\Delta E^*_{CIELAB} = \sqrt{(\Delta L^*)^2 + (\Delta a^*)^2 + (\Delta b^*)^2} \quad (12)$$

# 4. Spectrophotometer Measurement Geometries

Spectrophotometer measurements can differ depending on the geometry of the instrument, i.e., how the sample is illuminated and how t intensity of reflected light is measured. There are two main standard spectrophotometer geometries: bi-directional and integrating sphere. These are briefly described below; for more details see Ref. [1].

In bi-directional instruments the sample is illuminated at 0° and the reflected light is measured at 45° , or alternatively the sample is illuminated at 45° and the reflected light is measured at 0° . These are referred to as 0/45 and 45/0 geometries respectively, and the two are considered equivalent. All angles are measured relative to normal to the sample surface. Bi-directional spectrophotometers exclude any specularly reflected light very effectively because the detector angle is far from the specular angle.

In integrating sphere instruments the sample is diffusely illuminated and the reflected light is measured at 0 ° (D/0) or alternatively the sample is illuminated at 0 ° and the reflected light is measured after integrating at all reflected angles (0/D). Again these two are considered equivalent. An integrating sphere, which is a hollow sphere coated on the inside with a matte white material, is typically used either to provide the diffuse illumination or to collect the reflected light. There are two different ways in which D/0 or 0/D spectrophotometers can operate, depending on whether th specular component is included (IR) or excluded (XR). IR measurements include the specular component of the reflected light by placing a white cap at the specular reflection point in the integrating sphere, while XR measurements exclude the specular component of the reflection by replacing the white cap with a black one so that the specular reflection is absorbed. In spite of this, D/0-XR cannot completely exclude specularly reflected light unless the specular component is very sharp, because the detector angle is close to the specular angle.

Consequently, the reflected light reaching the detector consists of part or all of the diffusely reflected light and part or all of the specular reflected light, depending on the spectrophotometer geometry. Incomplete capture of the diffuse component is compensated for by calibrating the spectrophotometer relative to a perfect diffuse (Lambertian) reflector, in which case the quantity measured is the *reflectance factor*. Consequently the difference between measurements made with these spectrophotometer geometries is essentially limited to how much of specular component is detected. D/0-IR instruments capture virtually all of the specular component and 0/45 instruments capture almost none of it, while D/0-XR instruments lie somewhere between these extremes.

# 5. The Beer-Lambert Law

The Beer-Lambert Law[5] describes simple subtractive colorant mixing on a wavelength by wavelength basis considering the absorption of the incident light. The amount of incident light a color sample absorbs is said to depend on the thickness of the material as well as the concentration of the colorant with sample. The absorbance, *A*, of a sample at a particular wavelength is calculated according to equation 13.

$$A = a(\lambda)bc \quad (13)$$

The absorptivity, $a(\lambda)$, is a property of the colorant, the parameter *b* describes the thickness of the sample, and *c* is the concentration of the colorant within the sample.

The Beer-Lambert Law holds true in the absence of scattering.

# 6. Kubelka-Munk Color Model

Kubelka and Munk derived a color mixing model which describes the reflectance and transmittance of a color sample with respect to t absorption and scattering spectra of the material. Light is assumed to be diffuse in all directions after penetrating the sample, although the model simply considers the two net fluxes of straight up and straight down.

Along with the absorption spectrum, $K(\lambda)$, and scattering spectrum, $S(\lambda)$, the reflectance of a sample also depends on sample thickness, *X*, and the reflectance spectrum of the substrate or backing, $R_g(\lambda)$. What is commonly referred to as the exponential form of the Kubelka-Munk equation that is used to describe the reflectance of an object is given by equation 14. [3]

$$R = \frac{\frac{R_g - R_\infty}{R_\infty} - R_\infty\left(R_g - \frac{1}{R_\infty}\right)\exp\left[SX\left(\frac{1}{R_\infty} - R_\infty\right)\right]}{R_g - R_\infty - \left(R_g - \frac{1}{R_\infty}\right)\exp\left[SX\left(\frac{1}{R_\infty} - R_\infty\right)\right]} \quad (14)$$

The parameter $R_\infty$ represents the reflectance of an infinitely thick sample, which in turn is directly related to the absorption and scattering properties of the colorant in the following manner:

$$R_\infty = 1 + \frac{K}{S} - \sqrt{\left(\frac{K}{S}\right)^2 + 2\left(\frac{K}{S}\right)} \quad (15)$$

The spectra K and S can be fit to reflectance data as a function of wavelength over a series of mass or thickness points using the Kubelka-Munk equation.

If the scattering in a particular sample is negligible, the Kubelka-Munk model reduces to the Beer-Lambert Law.

## 7. Saunderson Correction Parameters

The Kubelka-Munk color model does not take into account the reflection losses at the sample boundaries. For example, the refractive i difference at the boundary between the sample and air gives rise to a certain amount of front surface reflection. The magnitude and angle a which this reflection is lost depend upon the gloss of the sample. Since a certain amount of light is lost to front surface reflection, thi illumination should be subtracted from the total amount of light illuminating the sample. Saunderson corrected for this loss of illumination for an integrating sphere measurement geometry with the correction parameter, $k_1$. The parameter $k_1$ depends on the refractive index of the two media comprising the surface, and can be calculated according to the Fresnel equations (Equations 1, 2, and 3) using the refractive index ratio of the two media and the angle of incidence of the illuminating light.[3]

Saunderson also accounted for a second loss of reflection within the sample. This loss occurs as the light travels downward through the sample, is reflected off the sample-substrate boundary and travels back upward toward the image-air boundary as if it were to re-emerge from the sample. However, a fraction of this light is again reflected off the image top surface back down into the sample and travels back sample-substrate boundary. This cycle may continue several times, and a fraction of the light, which Saunderson refers to as $k_2$, never re-emerges from the sample. $k_2$ can be calculated by integrating the Fresnel equations from 0 to 90 degrees under the assumption that the light becomes totally diffuse as soon as it enters the colorant layer. Since the reflectance loss calculated with the Fresnel equations greatly increase as the angle of incidence increases, the value of $k_2$ can become quite large (approximately 0.6 for toner on paper).

The corrected and measured reflectance that Saunderson derived taking these parameters into account for an integrating sphere measure geometry can be explained as follows. Table 1[2] shows the light leaving the boundaries of a sample for a single layer image for various cycles.

Table 1: Light leaving and arriving at image boundaries

| Cycle | Light leaving Air-Sample boundary and traveling Up | Light leaving Air-Sample boundary and traveling Down | Light arriving at Air-Sample boundary from Below |
|---|---|---|---|
| 1 | $k_1$ | $1-k_1$ | $(1-k_1)R_{corr}$ |
| 2 | $(1-k_1)(1-k_2)R_{corr}$ | $(1-k_1)k_2R_{corr}$ | $(1-k_1)k_2R_{corr}^2$ |
| 3 | $(1-k_1)(1-k_2)k_2R_{corr}^2$ | $(1-k_1)k_2^2R_{corr}^2$ | $(1-k_1)k_2^2R_{corr}^3$ |
| 4 | $(1-k_1)(1-k_2)k_2^2R_{corr}^3$ | $(1-k_1)k_2^3R_{corr}^3$ | $(1-k_1)k_2^3R_{corr}^4$ |

The amount of reflection that gets measured by the spectrophotometer can then be represented as the total light leaving the air-sample interfa and traveling up:

$$R_{measured} = k_1 + (1-k_1)(1-k_2)R_{corr}\left(1 + k_2R_{corr} + k_2^2R_{corr}^2 + \ldots\right)$$

From the relationship,

$$\sum_{q=0}^{\infty} a^q = 1 + a + a^2 + \ldots + a^n + \ldots = (1-a)^{-1}$$ ,

the measured reflectance that Saunderson defined can be rewritten as:

$$R_{measured} = k_1 + \frac{(1-k_1)(1-k_2)R_{corr}}{(1-k_2 R_{corr})} \quad (16a)$$

The corrected reflectance of the sample can also be solved for in terms of the Saunderson correction parameters, as is shown in equation 16b.

$$R_{corr} = \frac{R_{meas} - k_1}{1 - k_1 - k_2(1 - R_{meas})} \quad (16b)$$

where $R_{corr}$ is the reflectance described by the Kubelka-Munk color model.

# Model

## 1. Applications to Bi-directional Measurement Geometry

For xerographic color applications, it is often necessary to use a bi-directional measurement geometry system. Recall that the previously described Saunderson correction was derived for integrating sphere measurement geometry. Therefore, the Kubelka-Munk model with Saunderson correction needed modification for utilization with bi-directional measurement applications.

The adjustments to the model were made to account for the measurement of front surface reflection. The magnitude of the component that is specularly reflected depends on the image gloss and is reflected at an angle equal to the angle of illumination. The remainder of the front surface reflection is diffuse and assumed to be equally distributed over all angles.

With integrating sphere geometry, the detector collects all components of the front surface reflection. For 45/0 or 0/45 bi-directional measurement geometry, the detector of the spectrophotometer will not pick up all front surface reflection due to the geometric setup of the instrument. The detector will, however, read a portion of the diffuse front surface reflection. To account for this effect, a third correction parameter, $k_0$, was introduced. $k_0$ models the amount of front surface reflection that reaches the detector of the bi-directional measuring device.[7] The magnitude of $k_0$ is a function of image gloss. The segment of the diffuse front surface reflection that $k_0$ corrects for is illustrated in Figure 1.

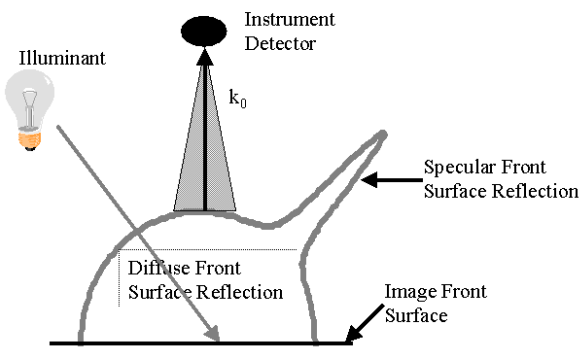


Figure 1: Illustration of the Correction Parameters $k_0$ and $k_1$

By accounting for this third correction parameter, the corrected and measured reflectance of a sample at any given wavelength may be described as follows:

$$R_{corr} = \frac{R_{meas} - k_0}{1 - k_1 - k_2 + k_1 k_2 - k_0 k_2 + k_2 R_{meas}} \quad (17a)$$

$$R_{meas} = k_0 + \frac{(1 - k_1)(1 - k_2) R_{corr}}{1 - (k_2 R_{corr})} \quad (17b)$$

For very high gloss samples measured using bi-directional measurement geometry, $k_0$ approaches 0 due to the fact that virtually all of the front surface reflection will be reflected at the specular angle, thus greatly reducing the diffuse portion which reaches the detector. At the other extreme, for integrating sphere geometry d/0 with specular included, $k_0=k_1$, and the equation reduces to equation 16 ("traditional" Saunderson correction). The method by which Equations 17a and 17b were derived is given in Appendix A at the end of this report.

# 2. Determining K and S for Individual Toners

The absorption (K) and scattering (S) spectra for each of the individual toners may be modeled using a toner mass series and the measured reflectance of each sample as a function of wavelength. A Method of Least Squares, as described in Appendix B, may be used to accomplish this. Correction parameters are applied to the measured reflectance before fitting the K and S spectra and the Kubelka-Munk equation is used with the corrected reflectance spectra determined with equation 17a. From the absorption and scattering spectra, the reflectance of a single toner layer of any known thickness may be predicted with respect to wavelength. The predicted reflectance is calculated using the absorption and scattering spectra with correction parameters $k_0$, $k_1$, and $k_2$ and equation 17b.

# 3. Method for Multilayer Images

The original Kubelka-Munk color model works well for single layer uniform images, but provides no method for application when more than one colorant layer is present, as is generally the case for process color xerographic print applications. A method was derived which uses the model to predict the reflectance of multiple layer images by treating each predicted layer reflectance as the substrate reflectance for the layer above it.

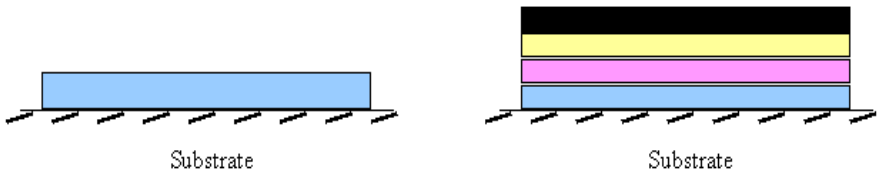


(a) (b)

Figure 2:

a. Single colorant layer considered in the original Kubelka-Munk model.
b. Multiple colorant layers (C, M, Y, K) generally encountered in process color xerographic prints.

An extension of the Kubelka-Munk color model was derived for predicting the reflectance of images with more than one toner layer. The method applies the Kubelka-Munk color model (via equation 14) to the bottom-most layer in the image. Before the substrate reflectance may be used to model the initial toner layer, the Saunderson correction (equation 17a) must be applied to the reflectance spectrum. Using the corrected reflectance spectrum of the bare substrate, along with the fitted absorption and scattering spectra of the material, the reflectance of the bottom-most layer may be modeled for a given toner thickness.

The reflectance spectrum that has been modeled for the first toner layer is then treated as the substrate reflectance spectrum, $R_p(\lambda)$, for the next toner layer in the image. The new "substrate" reflectance spectrum, along with the thickness and absorption and scattering spectra of the second material, may be input into the Kubelka-Munk model to predict the reflectance of the bi-layer image. The entire process is further repeated for all remaining layers in the image in order to model a final reflectance spectrum of a multi-layer sample.

After applying the Kubelka-Munk color model to all colorant layers in the image, the inverse of the Saunderson correction may be applied to convert the reflectance spectrum back to a measured reflectance space. The Inverse Saunderson calculation is illustrated in equation 17b.

The entire process for determining the reflectance spectrum of a multilayer image is illustrated in the following flow chart.

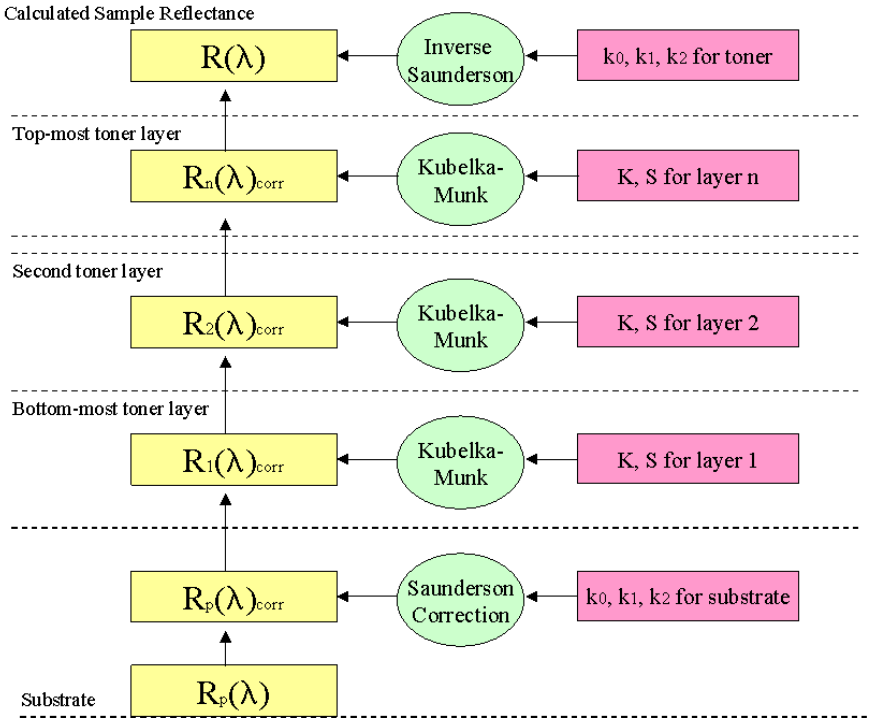


Figure 3: Flowchart illustrating the method for modeling the reflectance of a multilayer image

CIELAB values of the multi-layer image can be calculated by integrating the final predicted reflectance spectrum according to Equations 4-11.

## 4. Extension to NonPlanar Print Samples

Last, the established research in this area assumes the colorant layers in a particular color image to be smooth and uniform across the entire sample. This is often not true for xerographic color images. To account for these inconsistencies, a technique was developed which takes toner layer thickness variations into account when applying the Kubelka-Munk color model with correction parameters. To do so, print samples were cross sectioned and divided electronically into very small sections. Each section was chosen to be small enough so that if viewed independently of the rest of the cross section, all toner layers present in the image appeared to be planar. For cases in which the print layers are smooth, uniform, and planar, the Kubelka-Munk color model with Saunderson correction parameters works quite well. Therefore, the model was applied to each small, planar section of the image individually. To obtain a final reflectance spectrum, all sections were integrated over the entire image.

# Experimental

## 1. Sample Set

The complete form of the model was tested using a series of laboratory samples that spanned a wide range of toner mass values (0.35 mg/cm$^2$ – 2.0 mg/cm$^2$). These laboratory samples were chosen as a test set because the sample preparation procedure allows great control over deposited mass on the filter paper, resulting in very accurate control of toner mass per unit area. The laboratory sample preparation method also produces very smooth, uniform samples, which comply with the requirements of the Kubelka-Munk model.

These samples were prepared using cyan, magenta and yellow Xerox 5760 toners. Images were made at the following toner masses (TMAs): 0.35, 0.40, 0.45, 0.50, 0.60, 0.80, 1.0, 1.2, 1.6 and 2.0 mg/cm$^2$. Toner mass per unit area is related linearly to image thickness.

The laboratory prepared samples were fused on an off-line fuser. The fuser runs at a very slow speed resulting in a smooth, high gloss finish.

Toner pellet samples were used as infinitely thick data point approximations ($R\infty$) for each toner. Toner pellets of each of the color toners were made using a Carver Press and a brass circular mold. To make a pellet, approximately five grams of toner was weighed into the mold between two plungers, one fixed and one movable. The mold was then pressed to between 2500 and 3000 psi on the Carver Press. The result was an approximately 6mm thick disk of pressed toner. The toner pellet was then fused between two glass slides in a vacuum oven to remove air trapped in the sample and produce a smooth, glossy finish. The measured reflectance of the toner pellet is directly related to the absorption and scattering spectra of the material according to equation 15.

Multi-layer color laboratory samples were also prepared as layers of the primary toners. Unfused layers of the second color toner were transferred to an initial toner layer via heat and pressure. The bi-layer images were then fused on the off line fuser.

Print samples were imaged on a Xerox 5760 color printer which was chosen as the printer with which to print test / target images. The color of 100% coverage cyan, magenta, yellow, red, green, and blue patches were measured and designated as target colors. The color of the same patches were modeled using the described color model.

## 2. Color Measurements

All samples were measured on a Milton Roy ColorScan 45/0 spectrophotometer. The instrument illuminates the sample at an angle of 45 degrees and reads the reflectance factor at an angle of 0 degrees to the sample normal. CIELAB values were calculated for each measurement using D50 illuminant and 2° observer.

## 3. Image Photomicrographs

Image photomicrographs were completed on cyan, magenta, yellow, red, green, and blue 100% coverage patches from a test target printed on the Xerox 5760 color printer. The image photomicrographs are needed to examine and define the toner layer structure in each of the sample patches, and further allow extension of the Kubelka-Munk color model to xerographic print images. This layer structure needs to be defined due to the fact that the toner layer thickness may vary across a certain sample patch. Since layer thickness is used as input to the color model, a way to describe the fluctuations in layer thickness within a particular sample patch needed to be developed.

In order to examine the microscopic toner layer structure of xerographic print samples, the images were cross-sectioned and examined under high magnification. To prepare the cross section photographs, the images were cut at selected areas and embed in epoxy. Thin sections of each sample (1.5-2.5 microns) were microtomed and placed on a glass slide. To analyze each cross-section, the samples were examined with a Zeiss Axiomat microscope under high magnification (1965X). A Sony DXC-755 Camera was used to photograph each sample, and a Sony Color Video Printer (Mavigraph UP-5200MD) was used to print each photograph. A laboratory facility within Xerox Corporation was utilized to carry out the above procedure.

Examples of single layer (cyan) and multi-layer (blue) cross section photographs are shown below in figures 4 and 5.

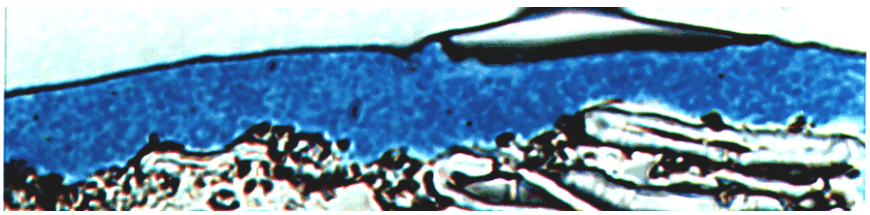

Figure 4: Image Cross Section of Single Layer Cyan 100% Coverage Sample Patch

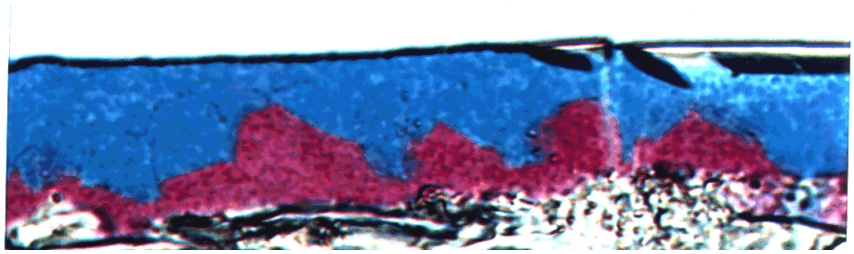

Figure 5: Image Cross Section of Multi Layer Blue 100% Coverage Sample Patch

1965X

## 4. Characterization of Toner Layer Structure in Hardcopy Print Images

From these types of cross section photographs, the variations in toner layer thickness across each print sample were characterized. Each photomicrograph was sectioned and divided into small sections across the entire image. The sections were divided into widths small enough that within each division the toner layers appear to be planar. For cases in which the print layers are smooth, uniform, and planar, the Kubelka-Munk color model with Saunderson correction parameters works quite well. Therefore, the model was applied to each small, planar section of the image cross section individually. To obtain a final reflectance spectrum, all sections were integrated over the entire image.

To section the print sample and measure the actual thickness of the toner layers in the image, the photomicrograph samples were electronically digitized to obtain an electronic reproduction of the image cross section in terms of x,y coordinate values. Electronic reproduction and digitization was accomplished with a HIPAD Digitizer. The HIPAD Digitizer is a compact digitizer with an active surface area of approximately 11X11 inches (28X28cm). A cursor or stylus is used as the input device. Each toner layer boundary was traced with the stylus to reproduce the layer structure of the image electronically. Readings were taken at intervals of 0.5 micron across the image. The ability to take readings at every 0.5 micron automatically divided the image into planar intervals.

# Results and Discussion

## 1. Determination of Saunderson Correction Parameters

To apply the model to actual samples, the correction parameters $k_0$, $k_1$, and $k_2$ need to be known for the toners of interest and for the substrates. The parameters are used to convert the measured reflectance to a corrected reflectance using equation 17a, and later to convert the corrected reflectance spectrum back to a "measured" reflectance spectrum through use of equation 17b.

Parameter $k_0$ is a measure of the amount of front surface reflection reaching the measuring device detector, which is positioned at a fixed angle. It is independent of wavelength but is a function of image gloss. $k_0$ will be equivalent for color toners within a set containing a common toner resin, provided that all the toners possess similar surface smoothing properties.

Parameter $k_0$ has been fitted for a 45/0 measurement geometry system as a function of TAPPI T-480 75° specular gloss. It was fitted for print samples which were made with Xerox 5775 toner (index of refraction $n$ =1.58) on five different coated and uncoated substrates and spanned a gloss range from 0 to 100gu. The fitted curve is referred to as r(g). It is described in detail in a paper describing the effect of gloss on image color. This paper has been submitted and is currently being reviewed for publication in *Color Research and Application.*

To calculate $k_0$ using this fitted curve, the 75° gloss of the laboratory and print samples was measured. The front surface reflectance factor, r(g), for the measured gloss value can be determined from the fitted curve. The following correction factor is then applied to account for the difference in the degree of front surface reflectance and surface smoothing properties due to the change in toner compositions between the toners.

$$k_0 = r(g) * \frac{F(n_2)}{F(n = 1.58)} \quad (18)$$

The F values represent the reflectance calculated using the Fresnel equations and the refractive indices of the air and the toner resin and the detector angle of the measurement device. $k_0$ was determined for the laboratory substrate and also for the Xerox 5760 images in this manner. The refractive index, $n_1$, of air was 1.0, the refractive index of the toner resin, $n_2$, was determined to be 1.58, and a 0° angle of illumination was used. For laboratory sample substrate, an $n_2$ value of 1.51 was used as the refractive index.

The Saunderson correction parameters $k_1$ and $k_2$ depend on the refractive index of the material and the angle of illumination. $k_1$ was calculated as the Fresnel reflectance for the indices of refraction mentioned above measured at the illumination angle of 0° . The parameter $k_2$ was determined by averaging the reflectance between 0° and 90° degrees using intervals of 0.2° .

The correction parameters calculated for the laboratory substrate and the Xerox 5760 toner set on laboratory substrate and Xerox Image Series LX paper are collected in Table 1.

Table 1: Correction Parameters for Xerox 5760 Test Set

| | $k_0$ | $k_1$ | $k_2$ |
|---|---|---|---|
| Laboratory Substrate | 0.030 | 0.052 | 0.573 |
| Xerox Image Series LX Substrate | 0.030 | 0.0413 | 0.573 |
| Xerox 5760 Toner on Laboratory Substrate | 0.000 | 0.0505 | 0.600 |
| Xerox 5760 Toner on Xerox Image Series LX Substrate | 0.0029 | 0.0505 | 0.600 |

## 2. Fitting K and S parameters

A method for finding the absorption and scattering spectra is described in detail in Appendix B. The measured reflectance of each data set was corrected using equation 17a and fit over the range of toner masses for each wavelength in the visual region of the spectrum, with each pellet reflectance input as a data point of infinite thickness. The laboratory sample substrate was also subjected to Saunderson correction and used as the paper reflectance. The resulting K and S spectra are shown in Figures 5 and 6.

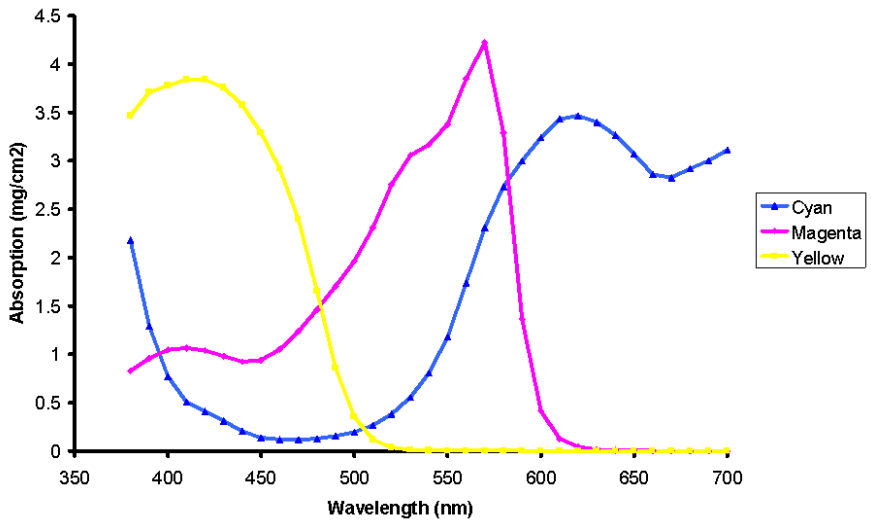


Figure 5: Absorption spectra of Cyan, Magenta and Yellow Xerox 5760 Toners

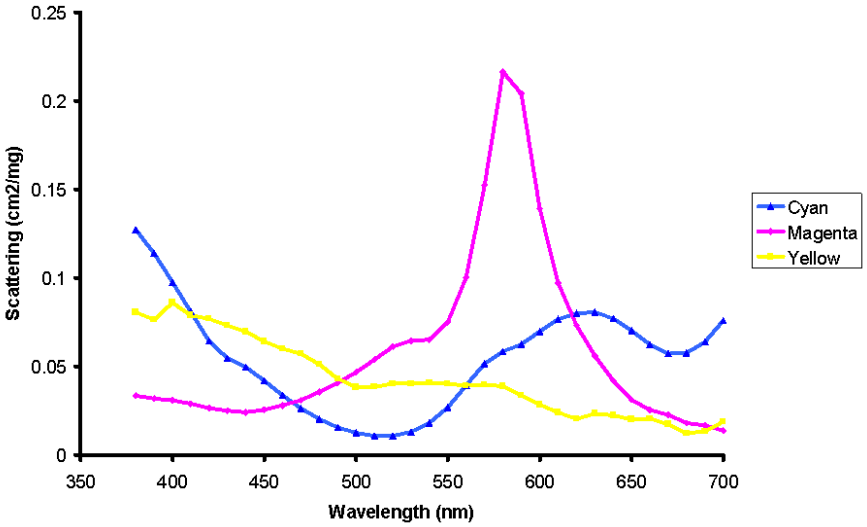


Figure 6: Scattering spectra of Cyan, Magenta and Yellow Xerox 5760 Toners

## 3. Modeling the Reflectance Spectra

As a test of the accuracy of the model, the absorption and scattering spectra of each toner were used to predict the measured reflectance spectrum for each toner mass in the TMA laboratory sample series, bi-layer red, green and blue laboratory samples and cyan, magenta, yellow, red, green and blue xerographic images. Equation 17a was used to correct the reflectance at each wavelength. Equations 14 and 15 were used to predict the reflectance, as a function of wavelength, in the corrected reflection domain at each toner mass value. Equation 17b was used to convert back to a measured reflectance domain.

## 4. Calculation of CIELAB Color Values

Equations 4 through 11 were then used to calculate the CIELAB values for each modeled reflectance spectrum using D50 illuminant and 2° observer. Each predicted color value was compared to a measured color value for the equivalent toner mass. $\Delta E^*_{CIELAB}$ was used as a measure of the difference between the predicted color that was determined using the model and the actual measured color values. Results for single layer laboratory samples modeled with 45/0 measurement geometry are summarized in Table 2.

Table 2: Color Difference between Predicted and Measured CIELAB values, Single Layer Laboratory images

| TMA ($mg/cm^2$) | Cyan $dE^*_{CIELAB}$ | Magenta $dE^*_{CIELAB}$ | Yellow $dE^*_{CIELAB}$ |
|---|---|---|---|
| 0.3 | | 1.32 | 2.81 |
| 0.35 | 2.87 | 1.68 | 1.77 |
| 0.4 | 0.83 | 1.12 | 3.31 |
| 0.45 | 2.87 | 1.49 | 1.13 |
| 0.5 | 1.6 | 0.83 | 1.58 |
| 0.55 | 1.81 | 0.25 | 0.82 |
| 0.6 | 2.49 | 0.31 | 0.88 |
| 0.8 | 0.88 | 2.59 | 0.76 |
| 1 | 1.55 | 1.7 | 0.78 |

| | | | |
|---|---|---|---|
| 1.2 | 1.81 | 2.77 | 0.94 |
| 1.6 | 0.66 | 4.07 | 0.72 |
| 2 | 2.77 | 4.93 | 0.94 |

The average color error between the modeled and measured color for single layers was $\Delta E^*_{AVG}$= 1.7. The corresponding RMS error for all single layer samples was 2.0.

# 5. Modeling of Multi-Layer Images

The same set of K and S parameters were used to predict the reflectance of red, green, and blue bi-layer images. The results were obtained by applying the Kubelka Munk color model with the appropriate correction parameters and by treating the predicted reflectance of the first (lower) toner layer as the substrate reflectance for the subsequent toner layer. Results were compared to measured red, green, and blue bi-layer images of the same TMA on wet deposition filter paper. Both measured and modeled CIELAB values were obtained for a 45/0 measurement geometry. Color difference values are shown in Table 4.

Table 4: Color Difference for bi-layer images

| Sample | dE* CIELAB |
|---|---|
| Red (Magenta / Yellow) | 2.5 |
| Green (Cyan / Yellow) | 3.0 |
| Blue (Cyan / Magenta) | 1.8 |

The average color difference for bi-layer images was $\Delta E^*_{AVG}$ = 2.4. The corresponding RMS error was 2.5.

Combining single and bi-layer data, the average color difference between the color predicted with the described model and the measured color was $\Delta E^*_{AVG}$ = 1.8, and the corresponding RMS error was 2.0

# 6. Extension to Nonplanar Print Samples

### 6.1 Thickness Probability

The digitizer was used to produce an electronic reproduction of each image photomicrograph by tracing all of the toner layer boundaries with the stylus. Readings were taken at every 0.5μ m in order to ensure each section was small enough so that it appeared planar on its own. The output obtained is an electronic set of x,y coordinates which define all layer boundaries present in the image as a function of position.

For each print sample, the thickness of each toner layer was determined as a function of position by subtracting y coordinate values at each corresponding x coordinate values across the print sample. A thickness probability function was defined to describe the likelihood that each toner thickness or combination of thickness' for two layer prints would occur. The probability was found to be the number of times each thickness, or combination of thickness pairs for double layer patches, occurred, divided by the total number of combinations that were tracked for the particular print.

$$P_i = \frac{N_{Thickness}}{N_{Total}} \quad (19)$$

A calculated probability function was then fit to the data points. For single color images, the normalized Gaussian function shown in Equation 20 was fit to the calculated probability data points.

$$P = A * \exp\left( -0.5 * \left( \frac{x - B}{C} \right)^2 \right) \quad (20)$$

where

$C = \frac{1}{A\sqrt{2\pi}}$, A and B are fitted constants, and x represents the image thickness.

The bi-layer probability functions were fit to a two dimensional "rotated" Gaussian equation of the form

$$P = \frac{1}{2\pi BD} \exp\left( -0.5 \left( \frac{x\cos(\theta) + y\sin(\theta) - A}{B} \right)^2 \right) \exp\left( -0.5 \left( \frac{(y\cos(\theta) - x\sin(\theta)) - C}{D} \right)^2 \right) \quad (21)$$

where x represents the thickness of layer 1, y represents the thickness of layer 2, θ is the angle of rotation, and A, B, C, D are fitted constants.

### 6.2 Application of the Kubelka-Munk Color Model

The Kubelka-Munk color model was used to predict the reflectance of each image. In order to predict the reflectance of the nonplanar images, the reflectance of all possible combinations of TMA values were predicted.

Since the measurements of the photographic cross sections were measured with respect to toner thickness, and the K and S spectra of the primary toners were modeled with respect to TMA, a conversion between toner thickness and sample TMA was needed. This relationship is characterized by fitting a straight line to the laboratory generated data, since the TMA is easily controlled and known in these images. The thickness of the layer is found using the image cross sections and measured via electronic digitization. A straight line relationship is characterized by examining a range of TMAs. For Xerox 5760 toners, the relationship is shown in Figure 7.

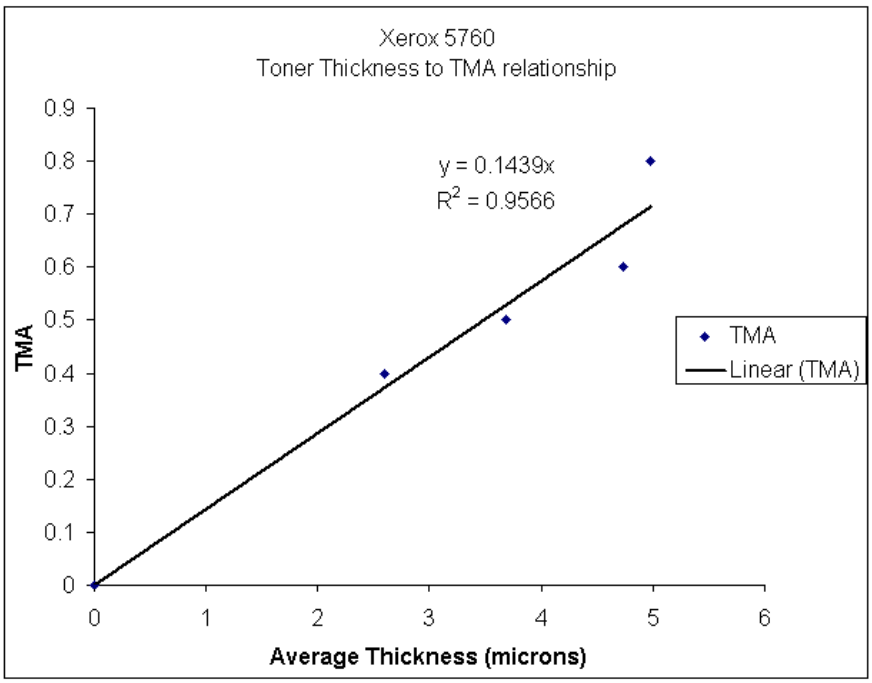


Figure 7: Linear Relationship between toner thickness and toner mass per unit area (TMA)

The reflection spectra for each thickness combination possible were calculated using the TMA from the converted thickness values, the K and S of each toner, and the Kubelka-Munk color model. The reflection spectra were further multiplied by the Gaussian probability function evaluated at the thickness values, and the products were then summed over all thickness value combinations between 0 and 10microns. A step size of 0.1 microns was used.

The reflection spectra were integrated according to equations 4-11 to obtain the CIELAB color values predicted using the described model. CIELAB color difference values between the predicted color and the actual measured color from the samples were used as a means to assess the accuracy of the model. Results are captured in Table 5.

Table 5: Color Difference for Xerographic 100% Coverage saturated images printed on a Xerox 5760 color printer

| Sample | dE* CIELAB |
|---|---|
| Cyan | 5.5 |
| Magenta | 5.2 |
| Yellow | 8.6 |
| Red | 4.48 |
| Green | 5.37 |
| Blue | 1.24 |

The average color difference for xerographic images was found to be 5.1 CIELAB units. The corresponding RMS error was 5.5.

# Conclusions

A method was demonstrated which extends the original Kubelka-Munk model to predict the reflectance of multi-layer images by treating the predicted reflectance of each toner layer as the substrate reflectance of toner layers above it. A procedure for applying the Saunderson correction for a bi-directional measurement geometry was also developed with the introduction of a third correction parameter, $k_0$. Last, a method was demonstrated which incorporates the characterization of an inconsistent toner layer thickness distribution into the developed color model.

The complete model was verified by testing with single and bi-layer toner and hardcopy print images measured using 45/0 measurement geometry. Results show the model to be quite accurate. Color difference ($\Delta E^*_{CIELAB}$) values between results predicted with the model and actual physical samples were used as a means to characterize the accuracy of the model. The average $\Delta E^*$ for single layer images was found to be 1.8 CIELAB units and the corresponding RMS error was 2.1. When testing the model with single and bi-layer harcopy print images, the average error between the modeled and measured color was found to be 5.1 CIELAB units, and the corresponding RMS error was 5.5.

Back to Contents

# References

1. P. Kubelka, "New Contributions to the Optics of Intensely Light-Scattering Materials. Part I," *J. Optical Society of America*, **38**, pp. 448-457 (1948).

2. E. Allen, "Colorant Formulation and Shading" in "Optical Radiation Measurements, Volume2," Academic Press, Inc., New York (1980).

3. D. B. Judd and G. Wyszecki, "Color in Business, Science and Industry," John Wiley, New York (1975).

4. J. L. Saunderson, "Calculation of the Color of Pigmented Plastics," *J. Optical Society of America*, **32**, pp. 727-736 (1942).

5. F. W. Billmeyer and M. Saltzman, "Principles of Color Technology," Second Edition, John Wiley, New York (1981).

6. *Colorimetry*, Second Edition, Publication CIE No. 15.2, Commission Internationale de l'Éclairage, Vienna (1986).

7. K. Natale, E. Dalal, "Modeling the Effect of Gloss on Color," **X9700251** (7/97).

Back to Contents

# Appendix A

A method similar to that described in Background Section 7 was used to determine the corrected and measured reflectance equations taking into account the third correction parameter, $k_0$. $k_0$ describes the front surface reflectance factor that must be considered when applying the Kubelka-Munk color model to a bidirectional geometry system.

Table A1 illustrates the amount of light entering and leaving various surfaces in a single layer sample.[2]

Table A1: Illustration of Light Leaving and Arriving at Sample Boundaries

| Light leaving sample-air boundary and travelling up | Light leaving sample-air boundary and going down | Light arriving at sample-air boundary from below |
|---|---|---|
| $k_1$ ($k_0$) | $(1-k_1)$ | $(1-k_1)\,R_{corr}$ |
| $(1-k_1)R_{corr}(1-k_2)$ | $(1-k_1)\,R_{corr}\,k_2$ | $(1-k_1)\,R_{corr}\,k_2\,R_{corr}$ |
| $(1-k_1)\,R_{corr}^2\,k_2(1-k_2)$ | $(1-k_1)\,R_{corr}^2\,k_2^2$ | $(1-k_1)\,k_2^2\,R_{corr}^3$ |
| $(1-k_1)\,R_{corr}^3\,k_2^2(1-k_2)$ | $(1-k_1)\,R_{corr}^3\,k_2^3$ | $(1-k_1)\,k_2^3\,R_{corr}^4$ |
| $(1-k_1)\,R_{corr}^4\,k_2^3(1-k_2)$ | $(1-k_1)\,R_{corr}^4\,k_2^4$ | $(1-k_1)\,k_2^4\,R_{corr}^5$ |
| $(1-k_1)(1-k_2)R_{corr}^n\,k_2^{n-1}$ | $(1-k_1)\,R_{corr}^5\,k_2^5$ | $(1-k_1)\,k_2^5\,R_{corr}^6$ |

From Table A1, the total light leaving the sample at the sample-air boundary and travelling up is:

$$R_{meas} = k_0 + \sum_{n=1}^{\infty}(1-k_1)(1-k_2)k_2^{(n-1)}R_{corr}^n \quad (1a)$$

Equation 1c can be rearranged and rewritten as:

$$R_{meas} = k_0 + (1-k_1)(1-k_2)R_{corr}\sum_{n=1}^{\infty}(k_2R_{corr})^{n-1} \quad (2a)$$

From the following relationship

$$\sum_{q=0}^{\infty}a^q = 1 + a + a^2 + \ldots + a^n + \ldots = (1-a)^{-1},$$

the relationship between the measured and corrected reflectance can be rewritten in final form as:

$$R_{meas} = k_0 + \frac{(1-k_1)(1-k_2)R_{corr}}{(1-k_2R_{corr})} \quad (3a)$$

The corrected reflection can then easily be solved for in terms of the measured reflectance and the correction coefficients. The steps to solve for it follow:

$$(R_{meas} - k_0) = \frac{(1-k_1)(1-k_2)R_{corr}}{(1-k_2 R_{corr})}$$

$$(R_{meas} - k_0)(1-k_2 R_{corr}) = (1-k_1)(1-k_2)R_{corr}$$

$$R_{meas} - R_{meas}k_2 R_{corr} - k_0 + k_0 k_2 R_{corr} = (1-k_1-k_2+k_1k_2)R_{corr}$$

$$R_{corr}(1-k_1-k_2+k_1k_2+R_{meas}k_2-k_0k_2) = (R_{meas}-k_0)$$

$$R_{corr} = \frac{(R_{meas}-k_0)}{1-k_1-k_2+k_1k_2-k_0k_2+R_{meas}k_2} \quad (4a)$$

Back to Contents

# Appendix B

To calculate the K and S parameters for a given toner set, the exponential form of the Kubelka-Munk equation may be used. This equation predicts the reflectance $R_i^0$ at a given wavelength: [3]

$$R_i^0 = \frac{\frac{R_p - R_\infty}{R_\infty} - R_\infty\left(R_p - \frac{1}{R_\infty}\right)\exp\left[SX\left(\frac{1}{R_\infty} - R_\infty\right)\right]}{R_p - R_\infty - \left(R_p - \frac{1}{R_\infty}\right)\exp\left[SX\left(\frac{1}{R_\infty} - R_\infty\right)\right]} \quad (1b)$$

where $R_p$ is the reflectance of the substrate or backing, $R\infty$ is the reflectance of an infinitely thick sample, S is the scattering coefficient at the given wavelength, and X represents the toner mass.

This can be rewritten as:

$$R_i^0 = \frac{R_p - R_\infty + R_\infty\left(1 - R_p R_\infty\right)\exp\left(2bSX_i\right)}{R_p R_\infty - R_\infty^2 + \left(1 - R_p R_\infty\right)\exp\left(2bSX_i\right)} \quad (2b)$$

where

$$b = \frac{1}{2}\left(\frac{1}{R_\infty} - R_\infty\right) . \quad (3b)$$

The mean square error of the reflectance predicted with the Kubelka-Munk model versus the measured reflectance for a given sample may be defined as follows, where $R_i$ is the measured reflectance:

$$E^2 \equiv \sum_i \left(R_i^0 - R_i\right)^2 \quad (4b)$$

$R_p$ and $R\infty$
can be determined by measuring the reflectance of the bare substrate and the toner pellet, respectively, and applying the Saunderson correction.

To solve for the S value at a particular wavelength which produces the lowest overall mean square error, $E^2$, the derivative of the mean square error with respect to S is set equal to zero. That is:

$$\frac{dE^2}{dS} = \sum_i \frac{d}{dS}\left(R_i^0 - R_i\right)^2 = 2\sum_i \left[\left(R_i^0 - R_i\right)\cdot\frac{dR_i^0}{dS}\right] \quad (5b)$$

Set the derivative equal to 0 to minimize $E^2$ with respect to S.

$$\frac{dE^2}{dS} = 2\sum_i \left[ \left(R_i^0 - R_i\right) \cdot \frac{dR_i^0}{dS} \right] = 0 \quad \text{(6b)}$$

Differentiating $R_i^0$ in equation 2b with respect to S:

$$\frac{dR_i^0}{dS} = \frac{d}{dS}\left( \frac{R_g - R_\infty - R_\infty\left(R_g R_\infty - 1\right)\exp\left(2bSX_i\right)}{R_g R_\infty - R_\infty^2 - \left(R_g R_\infty - 1\right)\exp\left(2bSX_i\right)} \right)$$

$$\therefore \frac{dR_i^0}{dS} = \frac{\left(R_g R_\infty - 1\right)\cdot\left(2bX_i\right)\exp\left(2bSX_i\right)}{R_g R_\infty - R_\infty^2 + \left(1 - R_g R_\infty\right)\exp\left(2bSX_i\right)}\left[R_i^0 - R_\infty\right] \quad \text{(7b)}$$

Substituting equation 7b into equation 6b

$$\frac{dE^2}{dS} = \left(R_g R_\infty - 1\right)\cdot\sum_i \frac{2bX_i \exp\left(2bSX_i\right)\left(R_i^0 - R_\infty\right)\left(R_i^0 - R_i\right)}{R_g R_\infty - R_\infty^2 + \left(1 - R_g R_\infty\right)\exp\left(2bSX_i\right)} = 0 \quad \text{(8b)}$$

The variables $R_p$, $R\infty$ , $X_i$, and b are all known quantities. The scattering coefficient S, which produces the lowest overall mean square error for the entire range of toner masses, for the given wavelength, can be determined from equation 8b using an iterative numerical procedure.

The following method can be used to obtain a good starting value for the iterative procedure to determine the S coefficient. The method avoids solving Equation 8b for inaccurate S values that may be obtained from local minima with respect to $E^2$. The following method determines the S coefficient for each wavelength that produces the overall minimum error.

Start with eq.(25) from Kubelka:[1]

$$SX = \frac{1}{b}\left[ \coth^{-1}\left(\frac{a - R}{b}\right) - \coth^{-1}\left(\frac{a - R_g}{b}\right) \right] \quad \text{(9b)}$$

Substitute the following equations:

$$\coth^{-1}(x) = \frac{1}{2}\ln\left(\frac{x+1}{x-1}\right) \quad \text{(10b)}$$

$$a + b = \frac{1}{R_\infty} \quad \text{(11b)}$$

$$a - b = R_\infty \quad \text{(12b)}$$

Substitution yields:

$$2bSX = \ln\left[\left(\frac{R_y - R_\infty}{1 - R_\infty R_y}\right)\cdot\left(\frac{1 - R_\infty R_i}{R_i - R_\infty}\right)\right] \quad (13b)$$

At this point, a initial starting value for S may be determined from defining a y axis in the following manner:

$$y = \ln\left[\left(\frac{R_y - R_\infty}{1 - R_\infty R_y}\right)\cdot\left(\frac{1 - R_\infty R_i}{R_i - R_\infty}\right)\right] \quad (14b)$$

If the above relationship is plotted as a function of X, where X is the sample TMA, the slope of the line can easily be solved for. From the slope and equation 14b, the initial guess of the S coefficient, $S_0$, for the wavelength of interest is as follows:

$$S_0 = \frac{slope}{2b} \quad (15b)$$

While this method produces a very good starting value, it is not suitable for the final fit, because of very low signal-to-noise ratio as $R_i \rightarrow R\infty$ . So the data has to be limited to high $R_i$. High $R_i$ occur at low toner masses at absorbing wavelengths, and at all toner masses at non-absorbing wavelengths. Therefore, a criterion was set such that $R_i - R\infty \geq \Delta$ , where $\Delta$ is some arbitrary positive fraction.

When the variable S is solved for, the following relationship between K and S can be used to determine K[1]:

$$\frac{K}{S} = \frac{(1 - R_\infty)^2}{2R_\infty} \quad (16b)$$

The absorption value, K, for each wavelength is therefore defined as:

$$K = \frac{K}{S}\cdot S = \frac{(1 - R_\infty)^2}{2R_\infty}\cdot S \quad (17b)$$

Back to Contents